Thesis for the Degree of Master of Engineering

Effects of Gelation Temperature on the Physical Properties of Calcium Alginate Gel Beads

by

Chungeun Jeong

Department of Food Science & Technology

The Graduate School

Pukyong National University

February 21, 2020

Effects of Gelation Temperature on the Physical Properties of Calcium Alginate Gel Beads

Calcium Alginate Gel Beads의 물리적 특성에 대한 겔화온도의 영향

Advisor: Prof. Seon-Bong Kim

by

Chungeun Jeong

A thesis submitted in partial fulfillment of the requirements
for the degree of

Master of Engineering

in Department of Food Science & Technology, the Graduate School,
Pukyong National University

February, 2020

Effects of Gelation Temperature on the Physical Properties of Calcium Alginate Gel Beads

A dissertation

by

Chungeun Jeong

Approved by

(Chairman) Suengmok Cho, Ph. D.

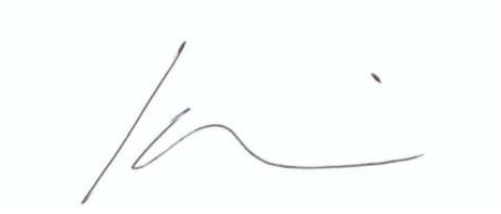

(Member) Young-Mog Kim, Ph. D.

(Member) Seon-Bong Kim Ph. D.

February 21, 2020

Contents

List of Tables

List of Figures

Calcium Alginate Gel Beads의 물리적 특성에 대한 겔화온도의 영향

정충은

부경대학교 대학원 식품공학과

요약

겔화온도는 calcium alginate gel (CAG) beads의 제조에서 중요한 인자이다. 하지만, CAG beads의 물리적 특성에 대한 겔화온도의 영향은 지금까지 많은 연구가 이루어지지 않았다. 이 연구에서 본인은 CAG beads의 물리적 특성(직경, 구형도 및 파열강도)에 대한 겔화온도 및 기타 주요 인자(sodium alginate와 calcium lactate의 농도 및 겔화시간)의 영향을 종합적으로 모니터링했다. 모니터링은 반응표면분석법을 사용하였으며 sodium alginate 농도(X_1, 1.2−3.6%, w/v), calcium lactate 농도(X_2, 0.5−4.5%, w/v), 겔화온도(X_3, 5−85 ° C) 및 겔화시간(X_4, 6−30 min)을 독립변수로, 직경(Y_1, mm), 구형도(Y_2, %) 및 파열강도(Y_3, kPa)를 종속변수로 설정하였다. CAG beads는 겔화온도 또는 겔화시간이 증가함에 따라 직경이 줄어들며 겔화온도가 낮아짐에 따라 파열강도가 증가했다. 또한, 5, 45 및 85 ° C에서 제조된 CAG beads 중에서 5 ° C에서 제조된 CAG beads는 가장 높은 파열강도(3976 kPa) 및 가장 낮은 칼슘함량(1.670 mg/g

wet)을 가졌으며 비교적 조밀하고 다공성이 적은 내부 구조를 관찰할 수 있었다. 이러한 결과는 겔화온도가 감소할 때 CAG beads에서 calcium 확산속도가 느려지고, 느려진 calcium 확산속도에 의해 보다 규칙적인 내부구조가 형성되고, 결과적으로 파열강도가 증가하는 것임을 보여준다.

Introduction

Calcium alginate gels (CAGs) have been used widely in various fields of biotechnology, including the food, medicine, and pharmaceutical industries, due to their biocompatibility, low toxicity, easy gel formation, and low price (Tavassoli-Kafrani, Shekarchizadeh, & Masoudpour-Behabadi, 2016). CAG formation is associated with the characteristic structure of alginate, a linear copolymer of 1,4-linked β-D-mannuronic acid and α-L-guluronic acid in which homopolymeric stretches of guluronic acid residues cooperatively bind calcium ions to form a three-dimensional gel structure, known as the egg-box model (di Cocco, Bianchetti, & Chiellini, 2003; Grant, Morris, Rees, Smith, & Thom, 1973; Grasdalen, Larsen, & Smidsrød, 1979; Smidsrød & Haug, 1972).

Generally, CAGs are prepared as a variety of beads or capsules (Vemmer & Patel, 2013); however, CAG beads are preferred over capsules as their preparation method is simpler. In the food industry, CAG beads can be used to effectively prepare imitation foods, particularly artificial fish roe (Ha, Jo, Cho, & Kim, 2016). The physical properties of CAG beads, such as rupture strength and sphericity, are very important for developing artificial fish roe and are influenced by preparation conditions including alginate and calcium concentrations, gelation temperature, and gelation time (Lee, Ravindra, & Chan, 2013). Many studies have investigated the effects of alginate and calcium concentrations on the physical properties of CAG beads (Martinsen, Skjåk Bræk, & Smidsrød, 1989; Ramdhan, Ching, Prakash, & Bhandari, 2019; Woo et al.,

2007); however, no previous studies have comprehensively investigated the effects of preparation conditions (sodium alginate and calcium lactate concentrations, gelation temperature, and gelation time) on the diameter, sphericity, and rupture strength of CAG beads. Although gelation temperature is an important factor for CAG bead preparation, few studies have examined its effects on the physical properties of CAG beads. For example, Yamagiwa, Kozawa, & Ohkawa (1995) demonstrated that compression strength increases as gelation temperature decreases from 55 to 5 °C, but failed to provide a detailed explanation for this observation.

In this study, we synthetically investigated the effects of gelation temperature (5 - 85 °C) and other factors on the physical properties (diameter, sphericity, and rupture strength) of CAG beads and comprehensively monitored these effects using response surface methodology (RSM) (Edwards & Jutan, 1997; Yolmeh & Jafari, 2017). RSM is a statistical technique used often for monitoring and optimization of food processing (Kim, Jeong, Cho, & Kim, 2019). It can describe the effect of independent variables on dependent variables and interrelationships among independent variables (Erbay & Icier, 2009). In this study, central composite design (CCD) was used for the design of experiments in RSM. The independent variables used this study were sodium alginate concentration (X_1, 1.2 - 3.6%, w/v), calcium lactate concentration (X_2, 0.5 - 4.5%, w/v), gelation temperature (X_3, 5 - 85 °C), and gelation time (X_4, 6 - 30 min), while diameter (Y_1, mm), sphericity (Y_2, %), and rupture strength (Y_3, kPa) were selected as the dependent variables. We also investigated the ion content and microstructure of CAG beads prepared at different gelation temperatures to investigate the effects of gelation temperature on the physical properties of CAG beads in more detail.

Materials and Methods

1. Materials

Sodium alginate (molecular weight: 220,000) and calcium lactate were purchased from Junsei Chemical Co., Ltd. (Tokyo, Japan) and Daejung Chemicals & Metals Co., Ltd. (Gyeonggi, Korea), respectively. Standard solutions for measuring sodium and calcium ion content were obtained from AccuStandard (1000 μg/mL in 2 - 5% nitric acid; Sodium ICP Standard, New Haven, USA) and PerkinElmer (100 μg/mL in 5% HNO3; Quality Control Standard-21 Elements, Massachusetts, USA), respectively. All other chemicals and reagents used were of analytical grade.

2. CAG bead preparation method

CAG beads were prepared according to the methods of Ha et al. (2016), with some modifications (Fig. 1). Sodium alginate solution was dropped into calcium lactate solution at a flow rate of 0.03 mL/sec through a single nozzle (19G, inner diameter: 0.80 mm, outer diameter: 1.10 mm) using a peristaltic pump (SMP-23, Eyela, Tokyo, Japan). The temperatures of the sodium alginate and calcium lactate solutions were controlled by a heating bath circulator (RBC-22, LABHOUSE, Gyeonggi, Korea) and a heating agitator, respectively.

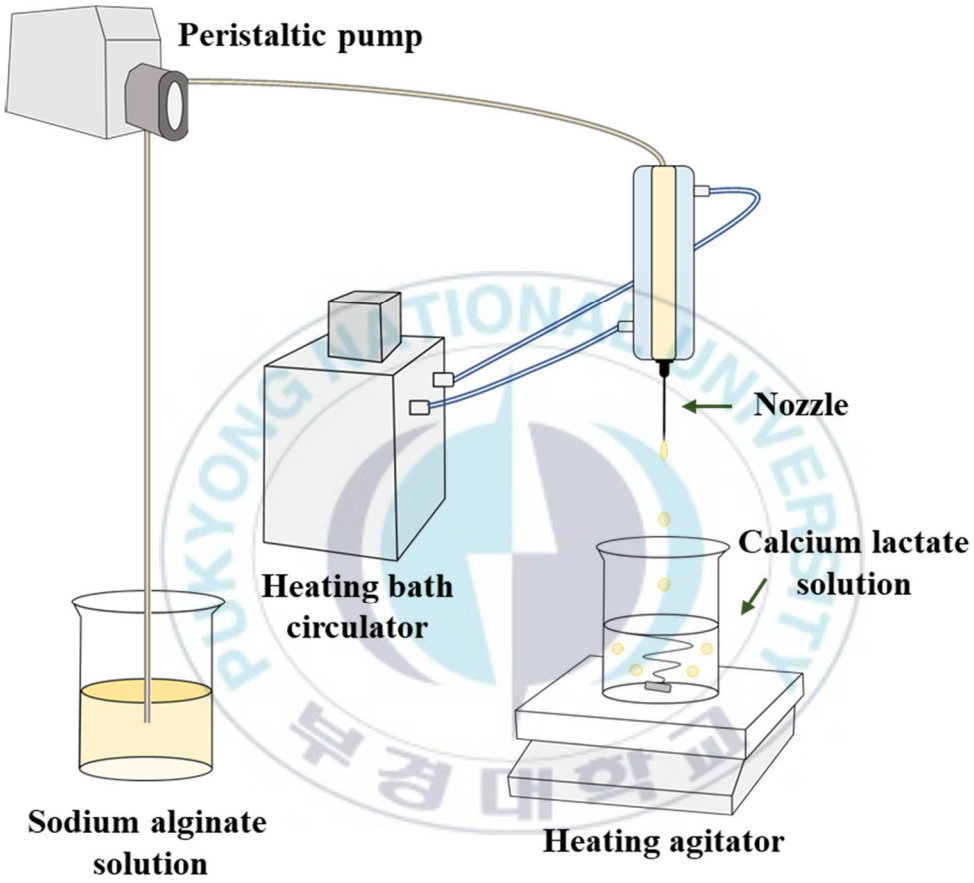

Fig. 1. Simple schematic diagram of CAG bead preparation.

Calcium lactate solution (250 mL) was agitated at a rate of 300 rpm in the reactor (500 mL). The drop distance from the single nozzle tip to the surface of the calcium lactate solution was 8 cm; therefore, the sodium alginate solution was affected by the room temperature (20 °C) while dripping into the calcium lactate solution surface, although it was difficult to measure this change accurately. We minimized the effect of room temperature by adjusting the outlet temperature of the sodium alginate solution from the nozzle to the gelation temperature. The prepared CAG beads were thoroughly washed with distilled water and used for analysis.

3. Diameter and sphericity measurement

To determine the diameter and sphericity of the CAG beads, we measured the shortest and longest diameter of ten randomly selected CAG beads with an image analyzer (i-SolutionTM 9.1, IMT i-Solution Inc., Daejeon, Korea) coupled to a stereoscopic microscope (125× magnification; SZX16, Olympus, Tokyo, Japan). The diameter (mm) of the CAG beads was calculated by averaging the shortest and longest diameters, while the sphericity (%) of the CAG beads was calculated as the percentage ratio of the shortest and longest diameters.

4. Rupture strength measurement

Rupture strength (kPa) is the maximum load applied to the sample area by a plunger when the sample is ruptured and permanently deformed. The rupture strength of the CAG beads (n = 10) was measured using a rheometer (Compac-100, Sun Scientific Co.,

Ltd., Tokyo, Japan) under the following conditions: MODE 4; adapter type, cylindrical plunger (diameter: 25 mm); penetration speed, 60 mm/min; correction, 0.2 N; and load-cell, 0.1 kN.

5. Experimental design and statistical analysis

Central composite design (CCD) was used to monitor the effects of different preparation conditions on the physical properties of CAG beads. The CCD matrix was composed to 2^4 factorial points, 2^3 axial points ($\alpha = 2$), and three replicates of the center point. The independent variables were sodium alginate concentration (X_1, %, w/v), calcium lactate concentration (X_2, %, w/v), gelation temperature (X_3, °C), and gelation time (X_4, min). The range of the independent variables and their levels are presented in Table 1. Diameter (Y_1, mm), sphericity (Y_2, %), and rupture strength (Y_3, kPa) were chosen as the dependent variables and the run order of the experiment was randomized to minimize unexpected variables. The experimental data were analyzed using the response surface regression procedure in Minitab statistical software (Version 16, Minitab Inc., Pennsylvania, USA) to fit the following generalized quadratic polynomial model equation (1):

$$Y = \beta_0 + \sum_{i=1}^{4} \beta_i X_i + \sum_{i=1}^{4} \beta_{ii} X_i^2 + \sum_{i=1}^{3} \sum_{j=i+1}^{4} \beta_{ij} X_i X_j \qquad (1),$$

where Y is the predicted dependent variable, β_0 is a constant, and β_i, β_{ii}, and β_{ij} are linear, quadratic, and interaction regression coefficients, respectively.

Table 1. The range and levels of the independent variables in CCD for monitoring the effects of preparation conditions on the physical properties.

Independent variables	Symbol	Range and levels				
		-2	-1	0	1	2
Sodium alginate concentration (%, w/v)	X_1	1.2	1.8	2.4	3.0	3.6
Calcium lactate concentration (%, w/v)	X_2	0.5	1.5	2.5	3.5	4.5
Gelation temperature (°C)	X_3	5	25	45	65	85
Gelation time (min)	X_4	6	12	18	24	30

X_i and X_j are coded values of the independent variables. Three-dimensional response surface plots were produced from the fitted response surface model equations using Maple software (Maple 7, Waterloo Maple Inc., Ontario, Canada).

6. Moisture content

The moisture content of the prepared CAG beads (n = 50) was determined using a digital moisture analyzer (MX-50, A&D, Tokyo, Japan) at 100 °C.

7. Calcium and sodium ion content

Inductively coupled plasma optical emission spectroscopy (ICP-OES; Avio 200, PerkinElmer, Massachusetts, USA) was used to measure calcium and sodium ion content. The dried CAG beads obtained after measuring the moisture content were collected and used as a dry sample for ICP-OES. The CAG bead preparation and drying process was repeated to collect approximately 0.3 g of dry sample for ICP-OES. Dry samples were completely dissolved in 2 mL ultrapure water, 4 mL nitric acid, and 0.5 mL hydrochloric acid using a microwave reaction system (Multiwave PRO, Anton Paar, Graz, Austria) and then deionized water was added to make 100 mL. The sodium ion content of the sample solution was measured at 589.592 nm by ICP-OES, while the calcium ion content was measured at 317.933 nm after the sample solution had been diluted 10-fold. Calibration curves were produced for 0 to 25 mg/L of calcium ions and 0 to 200 mg/L of sodium ions using standard solutions and used to determine the calcium and sodium ion content. The ion and moisture content of the dried CAG beads

were used to calculate the ion content of the wet CAG beads.

8. Sodium ions diffusion of CAG beads

CAG beads prepared at 5 ℃ were incubated with distilled water for 0, 30, and 60 minutes at room temperature to confirm whether the remaining sodium ions in the beads diffused out. The CAG beads were then immediately frozen in liquid nitrogen, cut in half, and lyophilized. An energy dispersive X-ray spectrometer (EDS; X-Max N, Oxford Instruments, Abingdon, UK) equipped with a field emission scanning electron microscope (FE-SEM; MIRA 3, TESCAN, Brno, Czech Republic) was used to analyze the sodium ion content of the dried CAG beads at an accelerating voltage of 15 kV.

9. CAG bead microstructure

A low vacuum scanning electron microscope (LV-SEM; JSM-6490LV, JEOL Ltd., Tokyo, Japan) was used to investigate the effect of gelation temperature on the microstructure of CAG beads. CAG beads prepared at each gelation temperature were frozen and dried using the method described in section 8, coated with gold using an ion sputter, and observed by LV-SEM at an accelerating voltage of 15 kV (E 1010, Hitachi, Tokyo, Japan).

Results and Discussion

1. Fitting the models

The CCD matrix and experimental values of the dependent variables for each independent variable are presented in Table 2. The experimental values were used to calculate the regression coefficients of the constant, linear, quadratic, and interaction terms in the quadratic polynomial model equations for each dependent variable. Tables 3 and 4 show the calculated coefficients and fitted equations, respectively. The constant and linear term coefficients for Y_1 (diameter) and Y_3 (rupture strength) were significant ($P < 0.05$), whereas the quadratic and interaction terms were not. The Y_2 (sphericity) constant, X_1, X_3, X_1X_1, and X_3X_3 term coefficients were significant ($P < 0.05$), but all interaction terms were insignificant. The determination coefficient (R^2) of the fitted quadratic polynomial model equations for Y_1, Y_2, and Y_3 were 0.913, 0.912, and 0.935, respectively, and the R^2 values for all response surface models were highly significant ($P < 0.01$; Cho, Gu, & Kim, 2005). These results indicate that the fitted equations adequately describe the effects of the independent variables on the diameter, sphericity, and rupture strength of CAG beads (Hashtjin & Abbasi, 2015).

Analysis of variance (ANOVA) was used to evaluate the quality of the fitted response surface model equations (Bezerra, Santelli, Oliveira, Villar, & Escaleira, 2008); the ANOVA results are shown in Table 5.

Table 2. The CCD matrix and experimental values of the dependent variables for each independent variable.

Run No.		Independent variables								Dependent variables		
		Coded values				Uncoded values						
		X_1	X_2	X_3	X_4	X_1	X_2	X_3	X_4	Y_1	Y_2	Y_3
Factorial portions	1	-1	-1	-1	-1	1.8	1.5	25	12	3.07	96.7	1993
	2	1	-1	-1	-1	3.0	1.5	25	12	3.08	98.9	3473
	3	-1	1	-1	-1	1.8	3.5	25	12	3.00	96.2	2274
	4	1	1	-1	-1	3.0	3.5	25	12	3.02	98.1	4005
	5	-1	-1	1	-1	1.8	1.5	65	12	2.82	92.1	1901
	6	1	-1	1	-1	3.0	1.5	65	12	2.88	95.4	2629
	7	-1	1	1	-1	1.8	3.5	65	12	2.81	91.6	2195
	8	1	1	1	-1	3.0	3.5	65	12	2.87	95.7	3606
	9	-1	-1	-1	1	1.8	1.5	25	24	2.93	97.8	2420
	10	1	-1	-1	1	3.0	1.5	25	24	2.99	99.2	3832
	11	-1	1	-1	1	1.8	3.5	25	24	2.91	98.3	2601
	12	1	1	-1	1	3.0	3.5	25	24	2.91	97.8	4500
	13	-1	-1	1	1	1.8	1.5	65	24	2.72	94.6	1959
	14	1	-1	1	1	3.0	1.5	65	24	2.77	95.5	3575
	15	-1	1	1	1	1.8	3.5	65	24	2.70	94.2	2087
	16	1	1	1	1	3.0	3.5	65	24	2.77	95.4	3902
Axial portions	17	-2	0	0	0	1.2	2.5	45	18	2.73	89.4	1436
	18	2	0	0	0	3.6	2.5	45	18	2.99	98.5	4420
	19	0	-2	0	0	2.4	0.5	45	18	3.14	96.6	1044
	20	0	2	0	0	2.4	4.5	45	18	2.82	98.1	3414
	21	0	0	-2	0	2.4	2.5	5	18	3.04	98.1	3976
	22	0	0	2	0	2.4	2.5	85	18	2.62	90.7	2440
	23	0	0	0	-2	2.4	2.5	45	6	3.09	96.7	2065
	24	0	0	0	2	2.4	2.5	45	30	2.88	97.8	3111
Center points	25	0	0	0	0	2.4	2.5	45	18	2.97	98.3	2788
	26	0	0	0	0	2.4	2.5	45	18	2.92	96.6	2942
	27	0	0	0	0	2.4	2.5	45	18	2.88	97.5	3110

X_1: Sodium alginate concentration (%, w/v), X_2: Calcium lactate concentration (%, w/v), X_3: Gelation temperature (°C), X_4: Gelation time (min).

Y_1: Diameter (mm), Y_2: Sphericity (%), Y_3: Rupture strength (kPa).

Table 3. The regression coefficients of the fitted quadratic polynomial models for monitoring the effects of preparation conditions on the physical properties.

Parameter	Y_1		Y_2		Y_3	
	Coefficient	*P*-value	Coefficient	*P*-value	Coefficient	*P*-value
Constant	2.92333	0.001	97.4667	0.001	2946.67	0.001
X_1	0.03542	0.011	1.3625	0.001	752.50	0.001
X_2	-0.03792	0.007	0.0042	0.986	338.67	0.001
X_3	-0.10042	0.001	-1.8042	0.001	-263.17	0.003
X_4	-0.05292	0.001	0.4292	0.088	203.83	0.013
X_1X_1	-0.01969	0.141	-0.8198	0.006	28.04	0.713
X_2X_2	0.01031	0.426	0.0302	0.904	-146.71	0.072
X_3X_3	-0.02719	0.050	-0.7073	0.014	98.04	0.212
X_4X_4	0.01156	0.373	0.0052	0.983	-56.96	0.459
X_1X_2	-0.00188	0.899	-0.0688	0.812	101.25	0.262
X_1X_3	0.00937	0.528	0.2813	0.340	-59.50	0.502
X_1X_4	0.00187	0.899	-0.5313	0.085	87.00	0.331
X_2X_3	0.01188	0.427	0.0938	0.746	4.00	0.964
X_2X_4	0.00187	0.899	0.0063	0.983	-48.75	0.581
X_3X_4	0.00062	0.966	0.1063	0.714	-26.00	0.767

X_1: Sodium alginate concentration (%, w/v), X_2: Calcium lactate concentration (%, w/v); X_3: Gelation temperature (°C), X_4: Gelation time (min).

Y_1: Diameter (mm), Y_2: Sphericity (%), Y_3: Rupture strength (kPa).

Table 4. The response surface model equations for monitoring the effects of preparation conditions on the physical properties.

Quadratic polynomial model equations	R^2	P-value
$Y_1 = 2.92333 + 0.03542X_1 - 0.03792X_2 - 0.10042X_3 - 0.05292X_4 - 0.01969X_1^2 + 0.01031X_2^2 - 0.02719X_3^2 + 0.01156X_4^2 - 0.00188X_1X_2 + 0.00937X_1X_3 + 0.00187X_1X_4 + 0.01188X_2X_3 + 0.00187X_2X_4 + 0.00062X_3X_4$	0.913	0.001
$Y_2 = 97.4667 + 1.3625X_1 + 0.0042X_2 - 1.8042X_3 + 0.4292X_4 - 0.8198X_1^2 + 0.0302X_2^2 - 0.7073X_3^2 + 0.0052X_4^2 - 0.0688X_1X_2 + 0.2813X_1X_3 - 0.5313X_1X_4 + 0.0938X_2X_3 + 0.0063X_2X_4 + 0.1063X_3X_4$	0.912	0.001
$Y_3 = 2946.67 + 752.50X_1 + 338.67X_2 - 263.17X_3 + 203.83X_4 + 28.04X_1^2 - 146.71X_2^2 + 98.04X_3^2 - 56.96X_4^2 + 101.25X_1X_2 - 59.50X_1X_3 + 87.00X_1X_4 + 4.00X_2X_3 - 48.75X_2X_4 - 26.00X_3X_4$	0.935	0.001

X_1: Sodium alginate concentration (%, w/v), X_2: Calcium lactate concentration (%, w/v), X_3: Gelation temperature (°C), X_4: gelation time (min).

Y_1: Diameter (mm), Y_2: Sphericity (%), Y_3: Rupture strength (kPa).

Table 5. The ANOVA of response surface model equations for monitoring the effects of preparation conditions on the physical properties.

Dependent variables	Sources	DF	SS	MS	*F*-value	*P*-value
Y_1	Regression					
	Linear	4	0.373817	0.093454	28.03	0.001
	Square	4	0.040404	0.010101	3.03	0.061
	Interaction	6	0.003838	0.000640	0.19	0.973
	Residual					
	Lack of fit	10	0.035942	0.003594	1.77	0.415
	Pure error	2	0.004067	0.002033		
	Total	26	0.458067			
Y_2	Regression					
	Linear	4	127.095	31.7738	24.74	0.001
	Square	4	25.677	6.4193	5.00	0.013
	Interaction	6	6.179	1.0298	0.80	0.587
	Residual					
	Lack of fit	10	13.967	1.3967	1.93	0.389
	Pure error	2	1.447	0.7233		
	Total	26	174.365			
Y_3	Regression					
	Linear	4	19002146	4750537	40.21	0.001
	Square	4	1093213	273303	2.31	0.117
	Interaction	6	390870	65145	0.55	0.760
	Residual					
	Lack of fit	10	1365918	136592	5.27	0.170
	Pure error	2	51875	25937		
	Total	26	21904022			

DF (Degrees of freedom), SS (Sum of square), MS (Mean square).

Y_1: Diameter (mm), Y_2: Sphericity (%), Y_3: Rupture strength (kPa).

The linear terms of all dependent variables were significant at the 99.9% probability level ($P < 0.001$) and the square term of Y_2 was significant ($P < 0.05$). Conversely, the square terms of Y_1 and Y_3 and interaction terms of all dependent variables were insignificant ($P > 0.05$). The P-values for the lack-of-fit tests of all response surface models were all higher than 0.05 (Y_1, Y_2, and Y_3 were 0.415, 0.389, and 0.170, respectively), suggesting that the response surface models adequately explain the functional relationship between the dependent and independent variables (Hadzir et al., 2016).

2. Diameter and sphericity

We used a three-dimensional response surface plot to visually display the effects of gelation temperature (X_3) and other independent variables [sodium alginate (X_1) and calcium lactate (X_2) concentration, gelation time (X_4)] on the physical properties of the CAG beads.

The diameter and sphericity of CAG beads are the most important physical properties that are visible to the naked eye when developing imitation foods such as artificial fish roe. Figure 2a shows that the diameter (Y_1) of the CAG beads increased with increasing sodium alginate concentration (X_1) and decreased with increasing gelation temperature (X_3). The effect of sodium alginate concentration and gelation temperature on the diameter of CAG beads may be explained by the viscosity of sodium alginate, which increased with increasing concentration or decreasing gelation temperature. As viscosity increased, the size of the sodium alginate droplets on the nozzle tip also increased, thereby increasing the diameter of the CAG beads (Florián-Algarín & Acevedo, 2010; Klokk & Melvik, 2002).

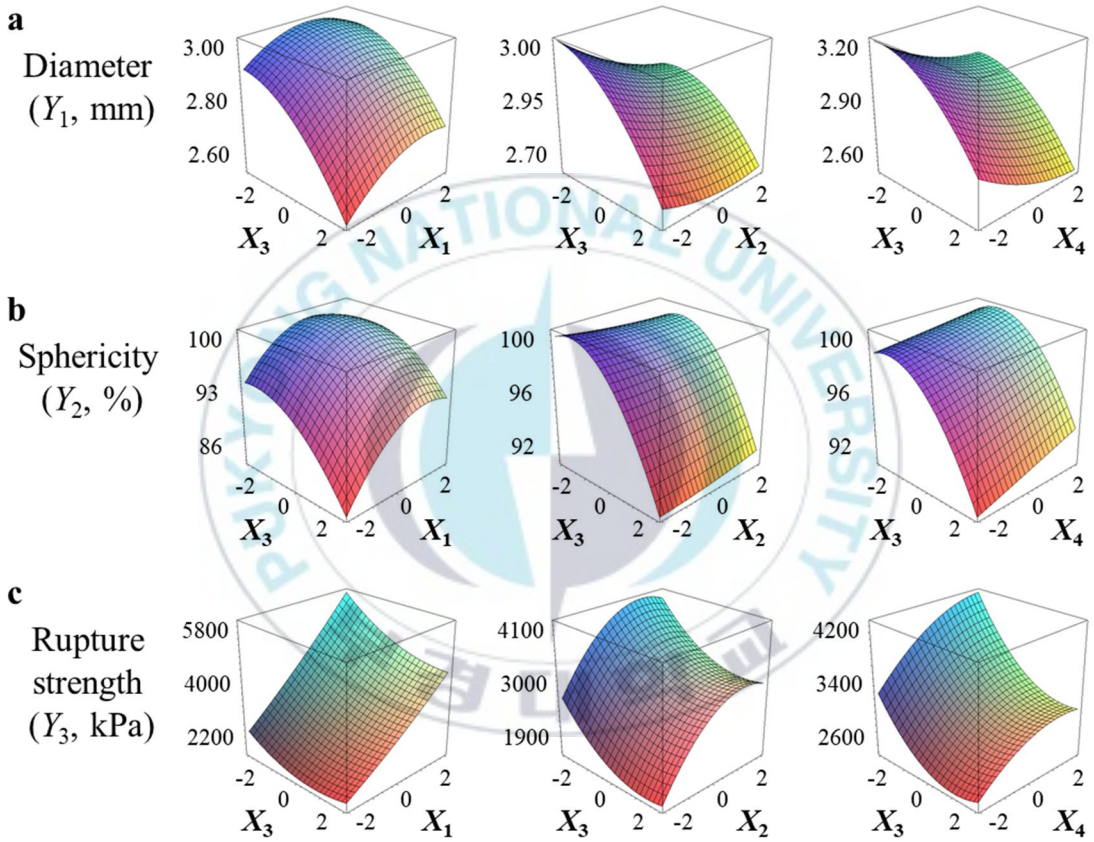

Fig. 2. Three-dimensional response surface plots of the physical properties of CAG beads. X_1, sodium alginate concentration (%, w/v); X_2, calcium lactate concentration (%, w/v); X_3, gelation temperature (°C); X_4, gelation time (min).

Moreover, it can be seen from Figure 2a that the diameter (Y_1) of the CAG beads decreased when the calcium lactate concentration (X_2) or gelation time (X_4) increased. These results can be explained by the study of Klokk & Melvik (2002), in which the gel network was contracted by diffusing calcium ions into the sodium alginate droplets in the reactor.

Figure 2b demonstrates that the sphericity (Y_2) of the CAG beads as increasing gelation temperature (X_3) increased slightly and then decreased gradually. This result contrasts with the effect of sodium alginate concentration on the sphericity of CAG beads. CAG bead sphericity is closely related to sodium alginate viscosity; the shape of sodium alginate droplets is significantly altered when they hit the calcium lactate solution surface under low viscosity conditions, but sphericity is recovered by increasing the surface tension and gelation above a certain viscosity (Lee et al., 2013). Consequently, the sphericity of the CAG beads gradually improved when sodium alginate viscosity increased (increasing sodium alginate concentration or decreasing gelation temperature); however, if the viscosity is too high, the falling sodium alginate droplets develop tails and the CAG beads eventually become tear-shaped (Li, Hou, Li, Zheng, & Li, 2013). Thus, the sphericity of the CAG beads is reduced slightly if the sodium alginate concentration is too high or the gelation temperature is too low. In this study, the CAG beads had a sphericity of around 94.6% at a sodium alginate concentration (X_1) of 2.4%, calcium lactate concentration (X_2) of 2.5%, gelation temperature (X_3) of 85 °C, and gelation time (X_4) of 18 min. Under these conditions, the CAG beads began to appear non-spherical when observed with the naked eye, but were indistinguishable from perfect spheres at a higher sphericity. Thus, preparation conditions must be carefully controlled to produce CAG beads with excellent visual sphericity.

3. Rupture strength

Rupture strength is an essential physical property of CAG beads that must be considered when imitating the texture of natural foods. Figure 2c shows that the rupture strength (Y_3) of CAG beads increased proportionally with to sodium alginate concentration (X_1), calcium lactate concentration (X_2), and gelation time (X_4). These results are consistent with previous studies that determined CAG gel strength according to the degree of interaction between calcium ions and α-L-guluronic acid, finding that strength was directly proportional to sodium alginate concentration, calcium concentration, and the duration of the interaction between alginate and calcium (Kaklamani, Cheneler, Grover, Adam, & Bowen, 2014; Mammarella, Vicin, & Rubiolo, 2002; Ramdhan et al., 2019).

Gelation temperature is an important factor that significantly affects the rupture strength of CAG beads but has not been studied in detail so far. As Figure 2c indicates, the rupture strength (Y_3) of the CAG beads increased when the gelation temperature (X_3) decreased. Some studies have hypothesized that the increase in gel strength with low gelation temperature may be caused by the formation of a more dense internal structure due to a reduced calcium ion diffusion rate (Augst, Kong, & Mooney, 2006; Drury, Dennis, & Mooney, 2004; Kuo & Ma, 2001); however, no experimental results or explanations yet support this theory. Consequently, we measured the calcium and sodium ion content of CAG beads prepared at 5, 45, and 85 °C with a 2.4% sodium alginate concentration, 2.5% calcium lactate concentration, and 18 min gelation time. As shown in Figure 3, the calcium ion content of the CAG beads decreased from 2.627 to 1.670 mg/g wet when the gelation temperature decreased from 85 to 5 °C.

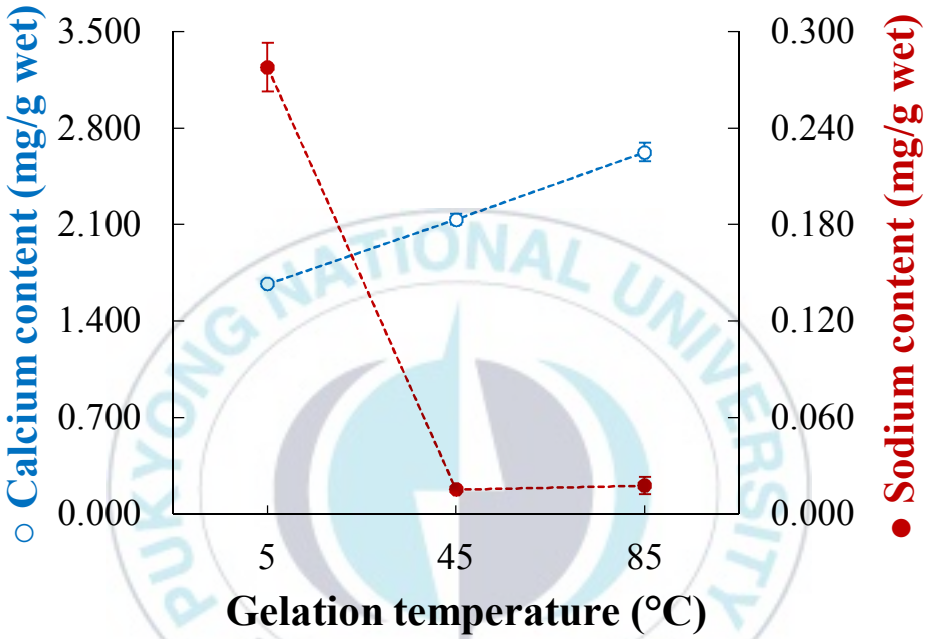

Fig. 3. Calcium (open circles) and sodium ion (filled circles) content of CAG beads prepared at different gelation temperatures.

These results indicate that the diffusion rate of calcium ions into sodium alginate droplets decreases with decreasing gelation temperature.

Moreover, the sodium ion content of the CAG beads was highest (0.278 mg/g wet) when the gelation temperature was 5 °C. This may cause the CAG beads to swell because of ion-exchange between the residual sodium and calcium ions and can be a problem for their storage stability (Bajpai & Sharma, 2004; Martinsen et al., 1989). We assumed that sodium ions may remain in the CAG beads' core, produced at a low gelation temperature because of a reduced diffusion rate out of the beads. Thus, we analyzed the distribution of residual sodium ions in CAG beads prepared at 5 °C and immersed in distilled water for 0, 30, and 60 min. Figure 4 shows that the residual sodium ion was detected in the core of the non-immersed CAG beads, but not in CAG beads immersed in distilled water for 30 or 60 min. These results indicate that sodium ions remain in the core of the CAG beads because the rate of ion diffusion slows down at low gelation temperatures. Furthermore, immersion allows sodium ion release, improving the storage stability of CAG beads prepared at low temperatures.

4. Microstructure

We investigated the effect of gelation temperature on the internal structure of CAG beads. To prevent excessive shrinkage during lyophilization and ensure easy cutting, the beads were lyophilized after being halved while frozen (Ayarza, Coello, & Nakamatsu, 2017; Voo, Ooi, Islam, Tey, & Chan, 2016). The CAG beads were prepared at a sodium alginate concentration, calcium lactate concentration, and gelation time of 2.4%, 2.5%, and 18 min, respectively.

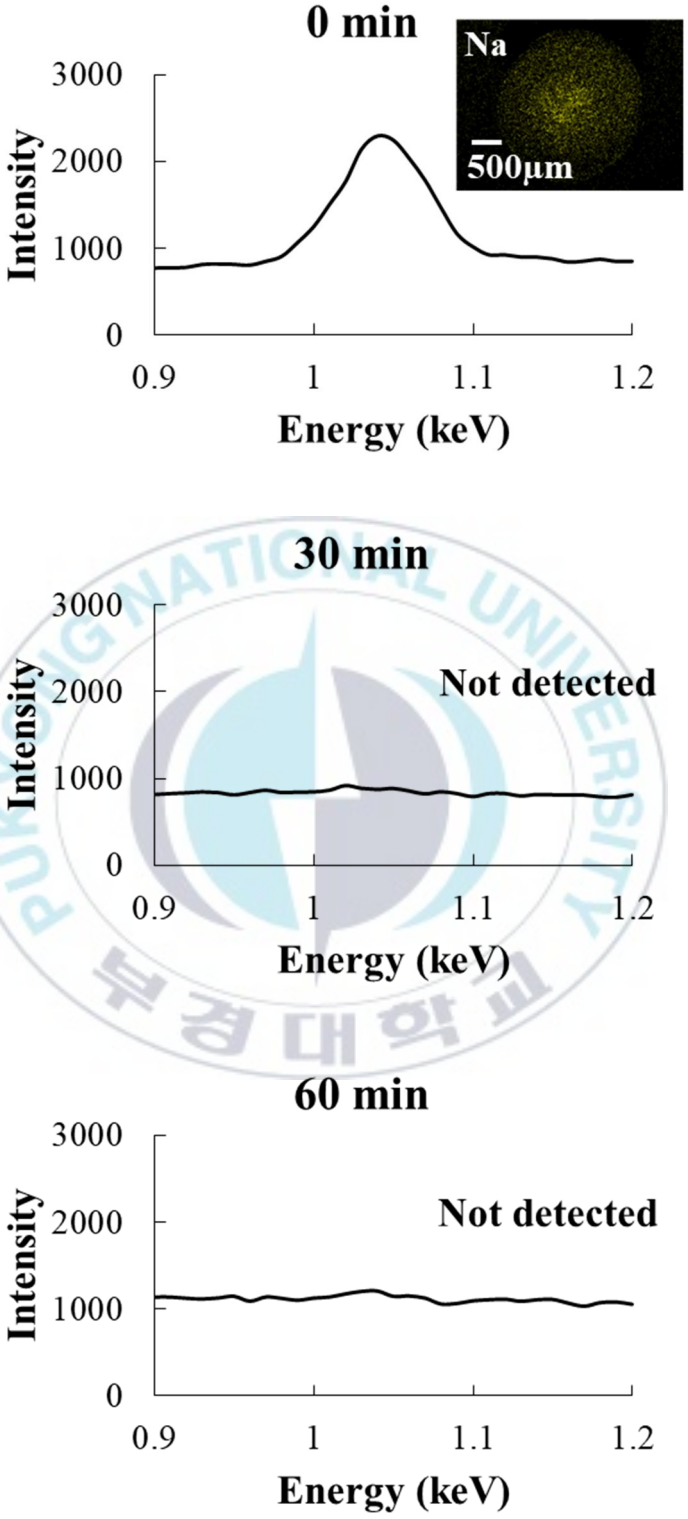

Fig. 4. EDS spectra and mapping results for sodium ions in CAG beads prepared at 5 °C after immersion in distilled water for different lengths of time.

Figure 5 depicts the internal structure of CAG beads prepared at gelation temperatures of 5, 45, and 85 °C. At 30× magnification, the CAG beads prepared at 85 °C had a smooth and homogeneous microstructure, whereas the beads prepared at 5 °C had a rough microstructure containing some big cracks which were likely caused when the CAG beads were freeze-dried due to the relatively high moisture content and rupture strength (Fig. 6). At 500× magnification, the CAG beads prepared at 5 °C displayed a microstructure with a well-connected bonding structure and a pattern, unlike those prepared at 45 and 85 °C. This regular microstructure is similar to the SEM image of CAG obtained by Topuz, Henke, Richtering, & Groll (2012). Furthermore, at 3000× magnification the CAG beads prepared at 5 °C had a dense, non-porous internal structure, whereas those prepared at 85 °C had an incomplete and pored microstructure. As mentioned above, the calcium ion diffusion rate increased with gelation temperature; therefore, the CAG beads prepared at a low gelation temperature had a more dense and regular internal structure, conferring increased rupture strength.

5. Optimal conditions for maximum rupture strength

Lastly, we optimized the conditions for preparing CAG beads with maximum rupture strength (Y_3). The optimal X_1 (sodium alginate concentration), X_2 (calcium lactate concentration), X_3 (gelation temperature), and X_4 (gelation time) conditions for preparing CAG beads with a maximum rupture strength were 3.6%, 4%, 5 °C, and 30 min, respectively (Table 6). Table 7 shows the percentage error verifying the accuracy of predicted values under the optimum conditions. The predicted Y_1 (diameter), Y_2 (sphericity), and Y_3 (rupture strength) values were 2.85 mm, 94.5%, and 6676 kPa, respectively. We prepared CAG beads under optimum conditions, yielding similar

experimental Y_1, Y_2, and Y_3 values of 2.88 ± 0.01 mm, 97.5 ± 0.9%, and 6444 ± 692 kPa, respectively. Consequently, the percentage error of this study is very small, meaning the developed models are suitable, while the predicted values agree with the experimental values (Whang et al., 2013).

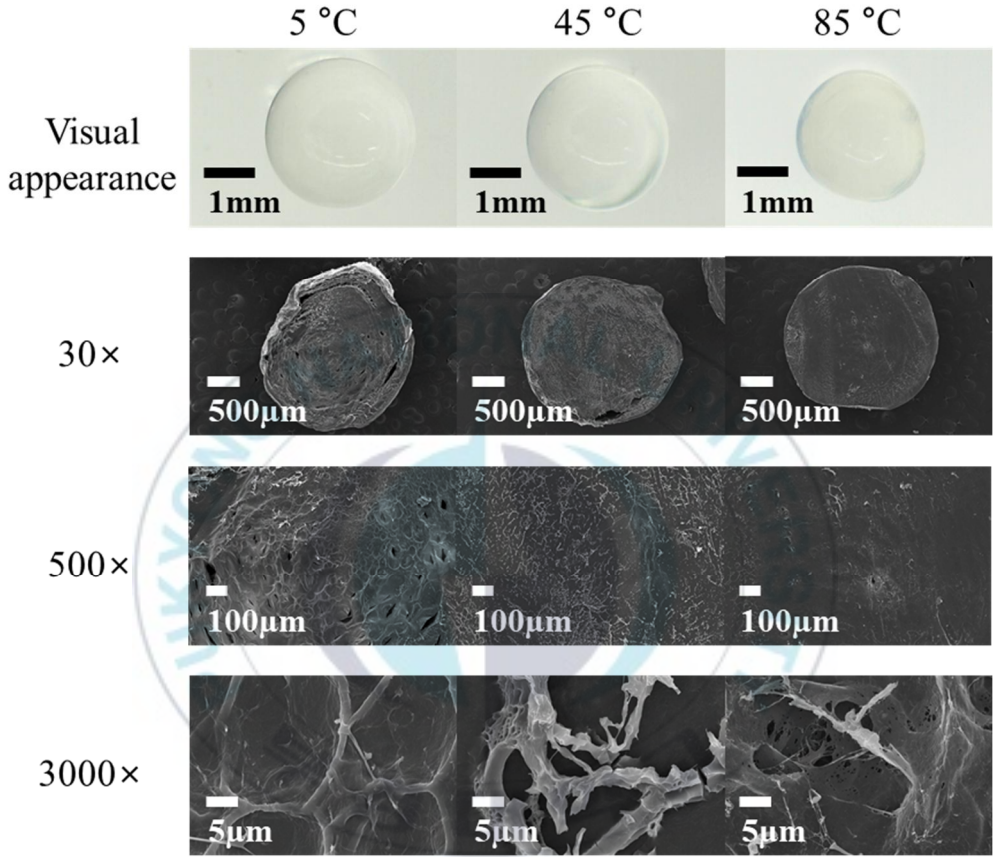

Fig. 5. Visual appearance and LV-SEM images of CAG beads prepared at different gelation temperatures.

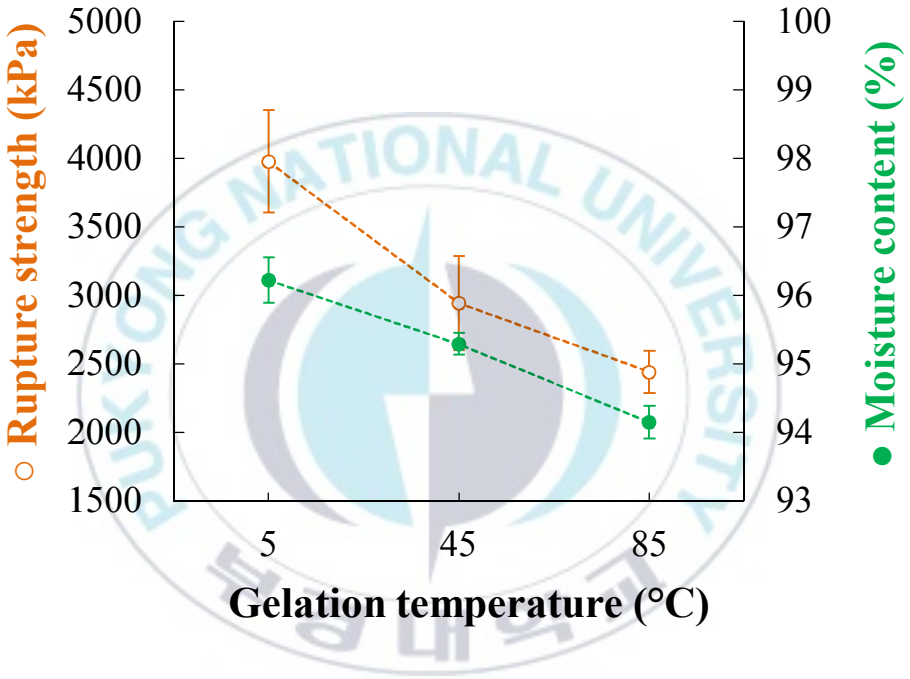

Fig. 6. Rupture strength (open circles) and moisture content (filled circles) of CAG beads prepared at different gelation temperatures.

Table 6. The optimal conditions for preparing CAG beads with a maximum rupture strength.

Optimal conditions			Y_3 Rupture strength (kPa)	
			Target value	Maximum
X_1 Sodium alginate concentration (%, w/v)	Coded value	2	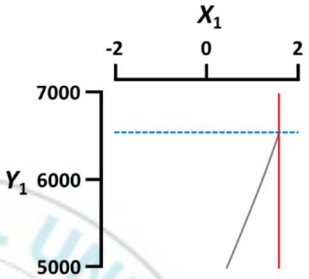	
	Actual value	3.6		
X_2 Calcium lactate concentration (%, w/v)	Coded value	1.5	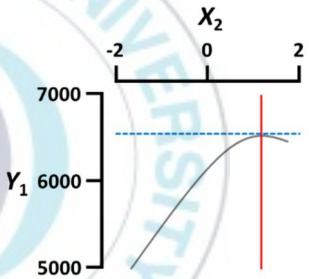	
	Actual value	4		
X_3 Gelation temperature (°C)	Coded value	-2	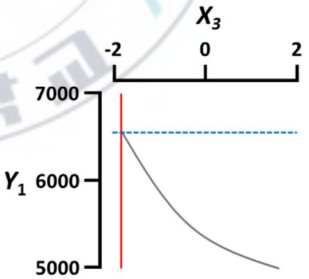	
	Actual value	4		
X_4 Gelation time (min)	Coded value	2	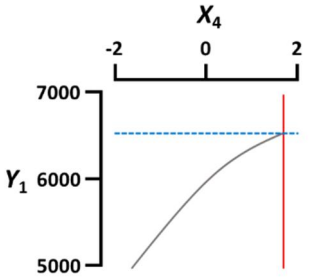	
	Actual value	30		

Table 7. Verification of experimental and predicted values under optimum conditions.

	Y_1 Diameter (mm)	Y_2 Sphericity (%)	Y_3 Rupture strength (kPa)
Predicted values	2.85	94.5	6676
Experimental values	2.88 ± 0.01	97.5 ± 0.9	6444 ± 692
Error (%)	1.05	3.17	3.48

Optimum conditions: Sodium alginate concentration = 3.6%; Calcium lactate concentration = 4% min; Gelation temperature = 4 °C; Gelation time = 30 min. Error (%) = (Difference among predicted value and actual value/predicted value) × 100.

Conclusions

In this study, we demonstrated that gelation temperature is an important factor affecting the physical properties of CAG beads. We found that the diameter, sphericity, and rupture strength of CAG beads are inversely proportional to gelation temperature. Moreover, low gelation temperatures slowed the calcium ion diffusion rate and resulted in CAG beads with a denser and more patterned microstructure, explaining why rupture strength increases as gelation temperature decreases. Furthermore, the CAG beads produced at a low gelation temperature may contain sodium ions, therefore immersion is necessary to release these ions and improve the storage stability of CAG beads. We suggest that gelation temperature should be considered carefully in future research and development using CAGs.

References

Augst, A. D., Kong, H. J., & Mooney, D. J. (2006). Alginate hydrogels as biomaterials. Macromolecular bioscience, 6(8), 623-633.

Ayarza, J., Coello, Y., & Nakamatsu, J. (2017). SEM–EDS study of ionically cross-linked alginate and alginic acid bead formation. International Journal of Polymer Analysis and Characterization, 22(1), 1-10.

Bajpai, S. K., & Sharma, S. (2004). Investigation of swelling/degradation behaviour of alginate beads crosslinked with Ca2+ and Ba2+ ions. Reactive and Functional Polymers, 59(2), 129-140.

Bezerra, M. A., Santelli, R. E., Oliveira, E. P., Villar, L. S., & Escaleira, L. A. (2008). Response surface methodology (RSM) as a tool for optimization in analytical chemistry. Talanta, 76(5), 965-977.

Cho, S. M., Gu, Y. S., & Kim, S. B. (2005). Extracting optimization and physical properties of yellowfin tuna (Thunnus albacares) skin gelatin compared to mammalian gelatins. Food Hydrocolloids, 19(2), 221-229.

di Cocco, M. E., Bianchetti, C., & Chiellini, F. (2003). 1H NMR Studies of Alginate Interactions with Amino Acids. Journal of bioactive and compatible polymers, 18(4), 283-296.

Drury, J. L., Dennis, R. G., & Mooney, D. J. (2004). The tensile properties of alginate hydrogels. Biomaterials, 25(16), 3187-3199.

Edwards, I. M., & Jutan, A. (1997). Optimization and control using response surface methods. Computers & chemical engineering, 21(4), 441-453.

Erbay, Z., & Icier, F. (2009). Optimization of hot air drying of olive leaves using response surface methodology. Journal of food engineering, 91(4), 533-541.

Florián-Algarín, V., & Acevedo, A. (2010). Rheology and thermotropic gelation of aqueous sodium alginate solutions. Journal of Pharmaceutical Innovation, 5(1-2), 37-44.

Grant, G. T., Morris, E. R., Rees, D. A., Smith, P. J., & Thom, D. (1973). Biological interactions between polysaccharides and divalent cations: the egg□box model. FEBS letters, 32(1), 195-198.

Grasdalen, H., Larsen, B., & Smidsrød, O. (1979). A pmr study of the composition and sequence of uronate residues in alginates. Carbohydrate Research, 68(1), 23-31.

Ha, B. B., Jo, E. H., Cho, S., & Kim, S. B. (2016). Production optimization of flying fish roe analogs using calcium alginate hydrogel beads. Fisheries and Aquatic Sciences, 19(1), 30.

Hadzir, M. H., Abbasiliasi, S., Ariff, A. B., Yusoff, S. B., Ng, H. S., & Tan, J. S. (2016). Partitioning behavior of recombinant lipase in Escherichia coli by ionic liquid-based aqueous two-phase systems. RSC Advances, 6(86), 82571-82580.

Hashtjin, A. M., & Abbasi, S. (2015). Nano-emulsification of orange peel essential oil using sonication and native gums. Food Hydrocolloids, 44, 40-48.

Kaklamani, G., Cheneler, D., Grover, L. M., Adams, M. J., & Bowen, J. (2014). Mechanical properties of alginate hydrogels manufactured using external gelation. Journal of the mechanical behavior of biomedical materials, 36, 135-142.

Kim, S., Jeong, C., Cho, S., & Kim, S. B. (2019). Effects of Thermal Treatment on the Physical Properties of Edible Calcium Alginate Gel Beads: Response Surface Methodological Approach. Foods, 8(11), 578.

Klokk, T. I., & Melvik, J. E. (2002). Controlling the size of alginate gel beads by use of a high electrostatic potential. Journal of microencapsulation, 19(4), 415-424.

Kuo, C. K., & Ma, P. X. (2001). Ionically crosslinked alginate hydrogels as

scaffolds for tissue engineering: Part 1. Structure, gelation rate and mechanical properties. Biomaterials, 22(6), 511-521.

Lee, B. B., Ravindra, P., & Chan, E. S. (2013). Size and shape of calcium alginate beads produced by extrusion dripping. Chemical Engineering & Technology, 36(10), 1627-1642.

Li, Z. Q., Hou, L. D., Li, Z., Zheng, W., & Li, L. (2013). Study on shape optimization of calcium–alginate beads. In Advanced Materials Research (Vol. 648, pp. 125-130). Trans Tech Publications.

Mammarella, E. J., De Piante Vicín, D. A., & Rubiolo, A. C. (2002). Evaluation of stress-strain for characterization of the rheological behavior of alginate and carrageenan gels. Brazilian Journal of Chemical Engineering, 19(4), 403-409.

Martinsen, A., Skjåk□Bræk, G., & Smidsrød, O. (1989). Alginate as immobilization material: I. Correlation between chemical and physical properties of alginate gel beads. Biotechnology and bioengineering, 33(1), 79-89.

Ramdhan, T., Ching, S. H., Prakash, S., & Bhandari, B. (2019). Time dependent gelling properties of cuboid alginate gels made by external gelation method: Effects of alginate-CaCl2 solution ratios and pH. Food hydrocolloids, 90, 232-240.

Smidsrod, O., & Haug, A. R. N. E. (1972). Dependence upon the gel-sol state of the ion-exchange properties of alginates. Acta chem. scand, 26(5), 2063-2074.

Tavassoli-Kafrani, E., Shekarchizadeh, H., & Masoudpour-Behabadi, M. (2016). Development of edible films and coatings from alginates and carrageenans. Carbohydrate polymers, 137, 360-374.

Topuz, F., Henke, A., Richtering, W., & Groll, J. (2012). Magnesium ions and alginate do form hydrogels: a rheological study. Soft Matter, 8(18), 4877-4881.

Vemmer, M., & Patel, A. V. (2013). Review of encapsulation methods suitable

for microbial biological control agents. Biological Control, 67(3), 380-389.

Voo, W. P., Ooi, C. W., Islam, A., Tey, B. T., & Chan, E. S. (2016). Calcium alginate hydrogel beads with high stiffness and extended dissolution behaviour. European Polymer Journal, 75, 343-353.

Wang, X., Chen, H., Liu, H., Li, P., Yan, Z., Huang, C., ... & Gu, Y. (2013). Simulation and optimization of continuous laser transmission welding between PET and titanium through FEM, RSM, GA and experiments. Optics and Lasers in Engineering, 51(11), 1245-1254.

Woo, J. W., Roh, H. J., Park, H. D., Ji, C. I., Lee, Y. B., & Kim, S. B. (2007). Sphericity optimization of calcium alginate gel beads and the effects of processing conditions on their physical properties. Food Science and Biotechnology, 16(5), 715-721.

Yamagiwa, K., Kozawa, T., & Ohkawa, A. (1995). Effects of alginate composition and gelling conditions on diffusional and mechanical properties of calcium-alginate gel beads. Journal of chemical engineering of Japan, 28(4), 462-467.

Yolmeh, M., & Jafari, S. M. (2017). Applications of response surface methodology in the food industry processes. Food and Bioprocess Technology, 10(3), 413-433.

Publications and Presentations

Publications

Jeong, C., Kim, S., Lee, C., Cho, S., & Kim, S. B. (2020). Changes in the Physical Properties of Calcium Alginate Gel Beads Under a Wide Range of Gelation Temperature Conditions. Foods (in review).

Oral presentations

November 1. 2018. Korean Federation of Fisheries Science and Technology Societies International Conference (in Korea)

Title: Effects of reparation conditions such as gelation temperature on physical properties of calcium alginate gel beads: A modeling study by response surface methodology

Poster presentations

October 24. 2019. The Korean Society of Food Science and Nutrition International Symposium and Annual Meeting (in Korea)

Title: Effects of Gelation Temperature on Physical Properties of Calcium Alginate Gel Beads

Acknowledgments

어느덧 2 년이라는 석사과정이 끝나고 학위논문을 제출하게 되었습니다. 석사과정 동안 학문적인 조언과 함께 앞으로 삶을 살아감에 있어 큰 가르침을 주신 김선봉 교수님께 감사의 말씀드립니다. 교수님 말씀처럼 머릿속의 쓸데없는 걱정은 훌훌 털어버리고 살도록 노력하겠습니다.

또한, 아직도 많이 부족하지만 저를 한명의 연구자로 거듭날 수 있도록 가르침을 주신 조승목 교수님께 감사를 드립니다. 그리고 저의 학부과정부터 석사과정까지 많은 가르침을 주신 조영제 교수님, 양지영 교수님, 이양봉 교수님, 전병수 교수님, 안동현 교수님, 김영목 교수님께 감사의 마음을 전합니다.

석사과정 동안 같이 동고동락한 정재연, 유정완, 그리고 동리형, 매번 귀찮게 연락 드려도 친절히 받아주고 술도 많이 사주신 홍덕형님, 걱정 많고 답답한 나랑 생활하느라 고생 많았던 석사 동기 성희, 해준 것 하나 없는 나한테 잘해준 모든 식품화학 실험실 식구들, 여기에 다 적을 순 없지만 20 살부터 함께 많은 추억을 쌓았던 식품공학과 형, 누나, 친구, 동생들 모두 저의 대학생활에 큰 힘이 되어 주신 것에 대해 감사의 마음 잊지 않겠습니다.

끝으로, 사랑하는 어머니, 아버지, 그리고 누나, 집에 잘 찾아 뵙지도 않은 불효자식 드디어 졸업합니다. 졸업까지 물심양면으로 지원해 주셔서 감사드립니다. 열심히 살아서 꼭 효도하겠습니다.